NJC

PAPER

View Article Online
View Journal

Cite this: DOI: 10.1039/c9nj03071a

Intramolecular hydrogen bond directed distribution of conformational populations in the derivatives of *N′*-benzylidenebenzohydrazide†

Neeru Arya, Sandeep Kumar Mishra and N. Suryaprakash *

Received 13th June 2019,
Accepted 25th July 2019

DOI: 10.1039/c9nj03071a

rsc.li/njc

Extensive investigation by 1D and various 2D NMR techniques revealed the presence of only *E* isomers with respect to the C=N bond and the existence of *cis*/*trans* conformations in the synthesized *N′*-benzylidenebenzohydrazide and its derivatives. The stable conformations of these molecules are attributed to the rotation of the molecular fragment around the C(O)–N bond. Interestingly, the conformational rigidity and the populations of the conformers are governed by the strengths of the intramolecular hydrogen bonds (HBs) between the *ortho* substituent on the benzoyl ring and the proton of the amide group, thereby permitting the architectural design of the preferred conformation of the molecules. The temperature perturbation studies and dilution studies using solvents of different polarities aided in the interpretation of inter- and intra-molecular HB interactions. The engagement of organic fluorine in the intramolecular HB is indubitably ascertained by the detection of the interaction strengths of a significant magnitude between organic fluorine and the NH proton, where the only mode of magnetization transfer between the interacting nuclei is HB ($^{1h}J_{FH}$). This is further endorsed by a physical parameter dependent perceivable variation in the strength of $^{1h}J_{FH}$. The weak molecular interactions are further ascertained by DFT based computations.

Introduction

The orbital symmetry, dynamics, electrostatic and stereoelectronic effects play a pivotal role in governing the conformation, reactivity and behavior of organic compounds. Consequently, a deeper understanding of the stereoelectronic and electrostatic effects aids in the logical design of reactions and functional molecular systems. Amongst various inter- and intra-molecular interactions, the weak HBs have drawn special attention and gained importance in chemistry, biology[1,2] and self-assembly of molecules.[3–7] The maximum number of reported intramolecular HBs are mainly N···H–N and O···H–N motifs.[8,9] Organic fluorine is very important in biomaterials, agrochemicals, molecular imaging,[10,11] crystal engineering[12] and also in the design of functional materials.[13] Conceptually it is well known that organic fluorine hardly ever gets involved in the intramolecular HB.[14–16] Nevertheless, since more than a decade, numerous experimental and theoretical reports have confirmed the participation of organic fluorine in intramolecular HB.[17–20] It is also well known that nearly 30% of the commercially available drugs contain at least one fluorine atom in their molecular fragment due to its binding nature with enzyme active sites[21,22] through HB interactions of the types, X–H···F–C (X = O and N). In addition, the strategic application to predictably control the molecular topology continues to remain elusive in the fields of pharmaceutical and biological chemistry.[23] Thus many groups have extensively investigated the HBs in molecules containing organic fluorine.

The different derivatives of benzylidenebenzohydrazides have exhibited their utilities as antimalarial,[24] cytotoxic,[25] antibacterial,[26] antihypertensive,[27] antioxidant,[28] antimicrobial,[29] antiviral,[30] antitumor[31] agents and in diverse areas of pharmacology. Thus, in the present study, we embarked on the synthesis and characterization of *N′*-benylidenbenzohydrazide and its derivatives. The synthesized compounds containing the azomethine group (–N=C<), with the desired substitution on the *ortho* position of the benzoyl ring, classified as *N′*-benzylidenebenzohydrazides that fall under the category of Schiff bases,[32] are investigated by the exploitation of 1D and 2D NMR techniques, supported by ESI MS, melting point and elemental analysis.

The chemical structures of the investigated molecules are reported in Scheme 1. All the experimental details are provided in the ESI.†

NMR Research Centre and Solid State and Structural Chemistry Unit, Indian Institute of Science, Bangalore 560012, India. E-mail: nsp@iisc.ac.in, suryaprakash1703@gmail.com; Fax: +91 8023601550; Tel: +91 8023607344, +91 8022933300, +91 9845124802

† Electronic supplementary information (ESI) available: One-dimensional ^{1}H NMR spectra, ^{13}C NMR spectra one-dimensional NOE spectrum, pseudo two-dimensional ^{1}H DOSY spectra and two-dimensional NOESY, EXSY spectra of the molecules; details of DFT based QTAIM and NCI studies; experimental details with the complete synthesis process and characterisation with ESI MS, melting point analysis, elemental analysis. See DOI: 10.1039/c9nj03071a

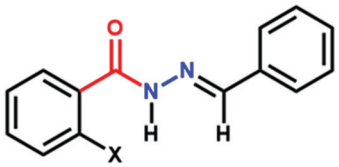

1. X=H
2. X=F
3. X=Cl
4. X=OH
5. X=OMe
6. X=CF_3

Scheme 1 The chemical structure of the derivatives of *N*′-benzylidene-2-X-benzohydrazide; X is the substituent on the benzoyl ring.

Results and discussion

The complete ^{1}H NMR spectra of compounds **1**, **2** and **4–6** are given in the ESI† (Fig. S1–S5). The spectrum of molecule **3** is shown in Fig. 1. On a close visual inspection of the spectra, one can notice the presence of two distinct peaks of the NH imide and CH vinyl protons. The chosen regions of the spectra of the NH protons of all the molecules are reported in Fig. 1i. It is evident from the figure that, for molecules **2**, **3** and **6** (their chemical structures given in Scheme 1), two distinct NH peaks of different intensity ratios were observed. On the other hand, a single peak is detected for the corresponding protons in molecules **1**, **4** and **5**.

To demystify the reason for such an observation, initially thorough NMR investigations were carried out on molecule **3**, which revealed two NH imide and CH vinyl proton peaks of nearly equal intensities. The corresponding 1D ^{1}H spectrum is reported in Fig. 1ii.

The first step is to find out whether the two NH peaks are from a single NH proton or from two different NH protons. Thus, an NMR spiking experiment with an equi-molar ratio (1 : 1) of compounds **3** and **5** was carried out. The corresponding spectrum is reported in the ESI† (Fig. S6). While calculating the molar ratio, it is assumed that molecule **3** has the expected chemical structure shown in Scheme 1. The integral area under the single NH peak of molecule **5** observed is exactly equal to the sum of the areas of both the NH peaks of molecule **3**. This strongly discards the presence of two NH protons. Consequent to a high signal overlap in the vinyl region, it was not possible to obtain accurate integral areas for these protons. However, the visual inspection of the intensities of the individual peaks reveals that they are nearly half compared to that of the vinyl proton of molecule **5**. These observations ascertain the structural framework of all the molecules reported in Scheme 1.

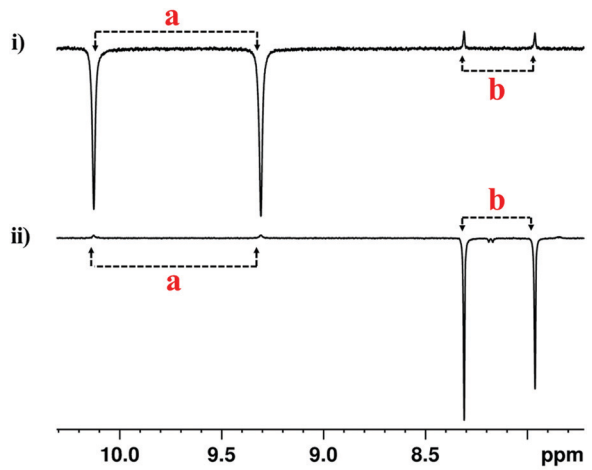

Fig. 2 400 MHz 1D nOe spectra of molecule **3**, in the solvent $CDCl_3$, at 298 K, where the proton was selectively excited; (i) at 9.3 ppm; and (ii) at 8.3 ppm. The NH imide and CH vinyl proton peaks are represented by alphabets a and b, respectively.

One cannot exclude the possibility that the observations from this spiking experiment could be identical if molecule **3** has a different structure with almost twice the molecular weight. To discern this, two-dimensional DOSY[33,34] experiments were carried out on two different samples, one with an equi-molar ratio (1 : 1) of compounds **3** and **5** (Fig. S7a, ESI†) and another with an equi-molar ratio of compounds **2**, **3** and **5** (1 : 1 : 1) (Fig. S7b, ESI†). The diffusion coefficients calculated from the DOSY spectra follow exactly the same order of the molecular weights as proposed in Scheme 1, discarding any possibility of the presence of different species for compound **3**.

In the subsequent step, we advanced towards explicating the reason for the two NH peaks of molecules **2**, **3** and **6**. For such a purpose 1D NOESY experiments were carried out on molecule **3**. The selective irradiation of an imide (NH) peak at 9.3 ppm resulted in the simultaneous excitation of both the NH peaks

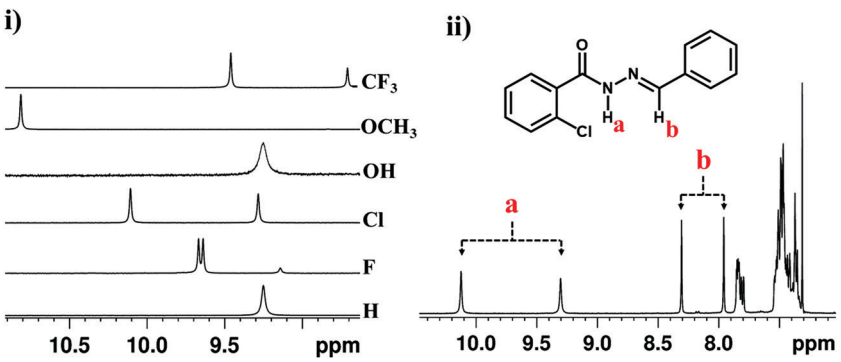

Fig. 1 400 MHz ^{1}H-NMR spectra of; (i) the selected NH regions of molecules **1–6** (from bottom trace to top trace); (ii) molecule **3** in the solvent $CDCl_3$ at 298 K. The concentration of the solution for each molecule is 10 mM, except for molecule **3**, which is nearly 15 mM. The NH imide and CH vinyl protons and their corresponding peaks in the ^{1}H spectrum are represented by alphabets a and b, respectively.

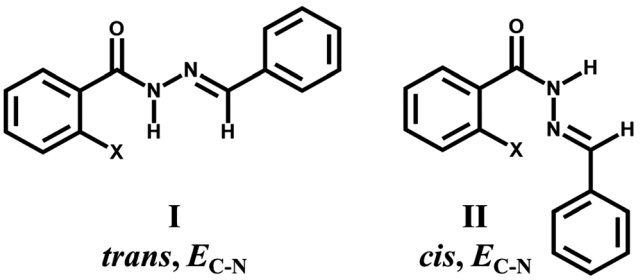

Fig. 3 Structures of the *trans*, E_{C-N} (**I**) and *cis*, E_{C-N} (**II**) conformers for *N*′-benzylidenebenzohydrazide derivatives.

and also exhibited a weak correlation with both the CH protons. The corresponding spectrum is reported in Fig. 2i. The observation of this phenomenon, especially when the two peaks are separated by a large chemical shift difference of nearly 0.8 ppm, is conceivable only when H/H exchange is occurring within the NMR time scale. This result suggests the presence of a single labile, exchangeable NH proton in the molecule. The 1D NOESY experiment with the selective excitation of a non-exchangeable vinyl proton (CH) resonating at 8.3 ppm (Fig. 2ii) also resulted in the simultaneous excitation of both CH peaks with a weak correlation to the NH peaks. Similar observations were also made for molecule **6,** whose spectrum is reported in the ESI† (Fig. S8). These observations immediately discard any possibility of NH proton exchange.

The other possible interpretation for the above observations could be the intermediate conformational exchange ($k_{exchange} = \Delta\omega$) between the molecules. To verify such a possibility, if any, a 2D EXSY (exchange spectroscopy) experiment was carried out on molecule **3** (Fig. S9, ESI†). The cross peaks observed in the EXSY spectrum between the two NH (imide) and two CH (vinyl) peaks confirmed the presence of conformational exchange on the NMR time scale.

For hydrazones, the possibility of the existence of *E*/*Z* geometrical isomers with respect to the C═N bond and *cis*/*trans* conformers at the C(O)–N bond has been discussed previously.[35,36] Due to restricted rotation about the C–N amide bond, the aromatic *N*-acylhydrazones exist as *E* isomers in solution.[36] In the present study also, the strong cross peaks observed between the NH imide proton and CH vinyl proton in the 2D NOESY spectrum confirmed that the investigated compounds exist only as *E* isomers about the C═N bond (Fig. S10 and S11, ESI†) and discarded the possibility of *Z* isomers. Consequent to steric hindrance, the possibility of a conformational change around the N–N is also excluded. Hence the only plausible reason for the observation of two sets of peaks for the NH imide and CH vinyl protons is attributed to the existence of conformers about the C(O)–N amide bond as *trans*, E_{C-N} (**I**) and *cis*, E_{C-N} (**II**) (Fig. 3).

Assignment of the *trans*, E_{C-N} (**I**) and *cis*, E_{C-N} (**II**) conformers can be interpreted as follows:

• Molecule **1** exhibits only a single peak consequent to the absence of intramolecular HB due to the absence of a substituent at the *ortho* proton of the benzoyl ring. As can be seen from the 2D NOESY spectrum of compound **1** (Fig. S10, ESI†), the cross peaks between the aromatic proton H_c and NH imide proton H_b confirms that molecule **1** exists as conformer **I**.

• Molecule **5** also exhibits only a single peak at a very high field due to the presence of a very strong HB. The cross peaks between the methoxy substituent and the NH imide proton H_a in the 2D NOESY spectrum of molecule **5** (Fig. S11, ESI†) confirms that molecule **5** also exists as conformer **I**.

• Molecules **2**, **3** and **6** show two peaks for the NH imide and CH vinyl protons with different intensity ratios pertaining to the presence of both conformers **I** and **II**. The intensity ratios depend strongly on the strength of the HB.

• In the case of molecule **2**, the F atom being a strong HB acceptor restricts the majority of the populations as conformer **I**. This can be clearly seen as the difference in the intensity ratios of both the conformers as shown in Fig. 1a. On the other hand, in molecules **3** and **6**, Cl and CF_3 being weak HB acceptors, result in the existence of both conformers **I** and **II** with noticeable intensity ratios (Fig. 1a).

• Molecule **4** contains the OH group, which can accept HB giving a single peak but nearly at the same chemical shift as that of molecule **1**. This is attributed to another possibility of

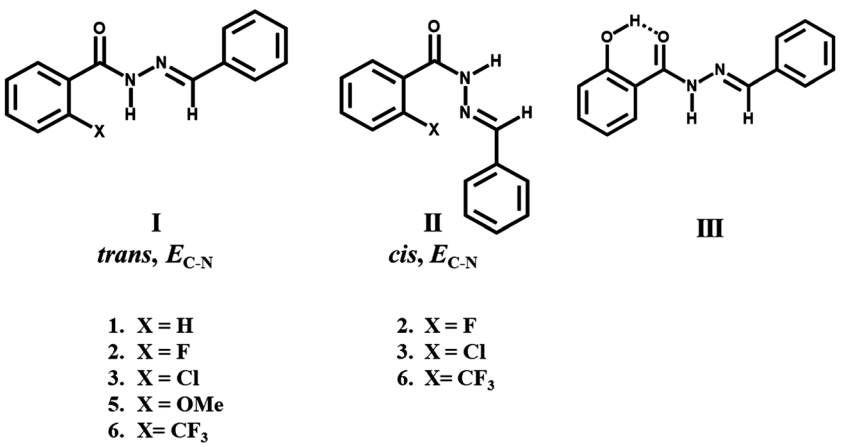

Fig. 4 Structures of all the possible conformers of molecules **1–6**. Molecules that exist in a particular conformer are mentioned below the conformational structures given.

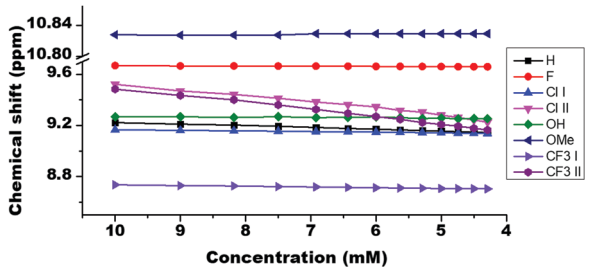

Fig. 5 The variation in the chemical shifts of the NH protons with decreasing solute concentration upon incremental addition of $CDCl_3$ to the solutions of compounds **1–6** (Fig. 1). Initially 10 mM concentration in 450 μL of $CDCl_3$ solvent was taken at 298 K and the solvent $CDCl_3$ was gradually added to it. The graphs for molecules **1–6** are represented by the symbols given in the inset. **I** and **II** correspond to the NH proton chemical shifts of conformers **I** and **II** of the Cl and CF_3 substituted molecules.

more favorable O–H···O=C type HB and no HB between oxygen and the NH proton in this molecule. Hence molecule **4** exists as conformer **III** (Fig. 4).

It is clearly evident from the above discussion that the conformational populations depend on the substituent (X) at the *ortho* position of the benzoyl ring, which can participate in HB with the NH proton. Another interesting observation is that the molecules with strong HB acceptor (*e.g.* molecules with substituent X with OCH_3) exist in only one conformation. Furthermore, the intensities of the two NH peaks correlate with the strengths of the HB between the substituent atom and the NH proton. These observations imply that the strengths of the HBs between the NH proton and the substituent on the benzoyl ring are controlling the conformational populations, in all the investigated compounds. The structures of possible conformers for all the molecules are reported in Fig. 4. The significant advantage is that it is possible to manipulate the strength of the intramolecular HB and restrict the molecule to a particular conformation or to obtain the desired ratio of two conformations. This can have numerous ramifications towards the selectivity, especially for enantioinduction in asymmetric synthesis,[37] and designing molecular switches.[38]

Effect of a solvent

Discrimination between inter- and intra-molecular interactions (HB)

To corroborate whether the HB is inter- or intra-molecular interaction and also to determine the effect of monomeric water on it, dilution studies with solvent $CDCl_3$ were performed on compounds **1–6**.[39–41] The plot of the chemical shift change with gradual addition of $CDCl_3$ solvent is reported in Fig. 5. The downfield shift for the NH proton is expected if the intermolecular HB is present. The chemical shift displacement of the water peak, if any, indicates the interaction between the water and hydrogen bonding sites in the compounds. The ^1H chemical shift of the water protons remained nearly same upon dilution, substantiating the negligible effect of monomeric water on the interactions present in the system.[42]

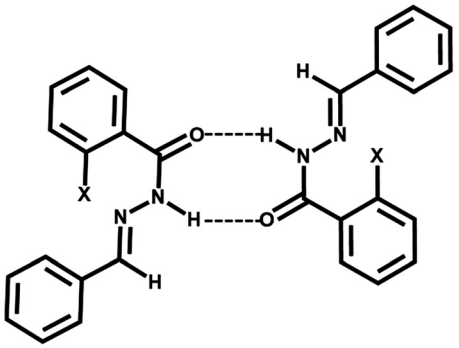

Fig. 6 Formation of intermolecular HB among the conformers **II**.

There is no significant variation in the chemical shifts of the NH proton except for conformer **II** of molecules **3** and **6**, which is evident from Fig. 5, thereby discarding any possibility of aggregation or the intermolecular HB for the rest of the molecules. Since Cl is a very weak HB acceptor and the HB formed by CF_3 is transient due to the free rotation of this group, molecules **3** and **6** exist in two conformers, out of which conformer **I** follows the same trend as the rest of the molecules. On the other hand, conformer **II** of both these molecules is showing variation in the chemical shift upon dilution with $CDCl_3$. The NH proton in conformer **II** is free and exposed to participate in the C=O···HN type intermolecular HB between themselves in $CDCl_3$ solvent (Fig. 6). This results in the shielding of the NH proton chemical shift with dilution (Fig. 5, inset symbols Cl **II** and CF_3 **II**). Upon a close visualization of the plots shown in Fig. 5, a little upfield chemical shift change in the NH proton of unsubstituted molecule **1** is also observed upon dilution (Fig. 5, inset symbol H). Since molecule **1** exists as conformer **I**, the NH proton is exposed, and consequent to the absence of any intramolecular HB, it may be attributed to intermolecular HB. The temperature dependent study discussed in the later part of the manuscript agrees with this interpretation.

Relative strengths of the HBs: a qualitative comparison

Dimethyl sulphoxide (DMSO) solvent, due to its high polarity, serves as a good HB acceptor and can breach various types of inter- and intra-molecular HBs by establishing strong interactions.[43,44] Hence it was used for the qualitative comparison of the relative strengths of the interactions. For such a purpose, titration with the solvent DMSO-d_6 was carried out on compounds **1–6**. Fig. 7 shows the plots of the chemical shift variation with the addition of DMSO solvent.

The excessive downfield displacement for NH resonances is observed in all the investigated compounds, except molecule **5**, where the substituent is the methoxy group, which is a very strong HB acceptor and impedes the rupture of the intramolecular HB by DMSO. The extent of the downfield displacement with respect to the volume of DMSO is directly related to the strength of the intramolecular HB. It is smaller for stronger interactions and comparatively larger for the weaker ones. The chemical shift values of the NH imide, CH vinyl proton and percentages of conformers **I** and **II** for molecules **1**, **2**, **3**, **5** and **6**

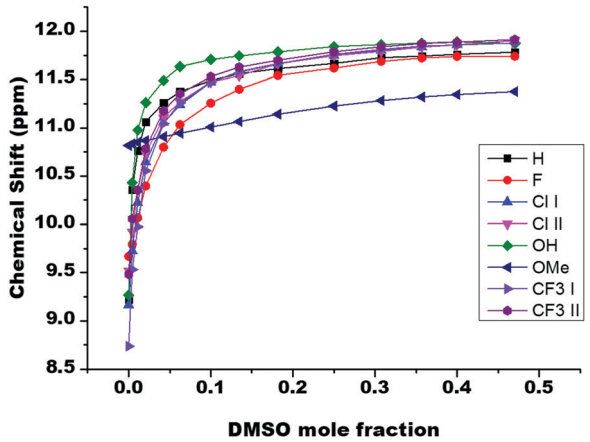

Fig. 7 The chemical shift variation of the NH protons with gradual addition of DMSO-d_6, for compounds **1–6**. Initially 10 mM concentration in 450 μL of $CDCl_3$ solvent was taken at 298 K and the solvent DMSO-d_6 was gradually added to it. Molecules **1–6** (Scheme 1) are marked by the symbols given in the inset. **I** and **II** in the inset correspond to the NH proton chemical shifts of conformers **I** and **II** of the Cl and CF_3 containing molecules.

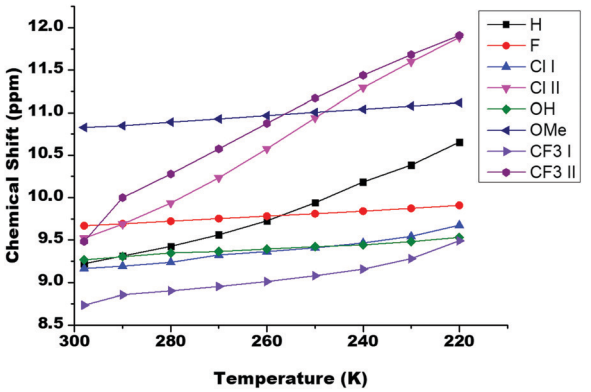

Fig. 8 NH proton chemical shift changes with temperature variation for compounds **1–6**. The concentration was 10 mM in the $CDCl_3$ solvent. The molecules are represented by the symbols given in the inset. **I** and **II** in the inset correspond to the NH proton chemical shifts of conformers **I** and **II** of the Cl and CF_3 containing molecules.

in $CDCl_3$ and DMSO solvents are compiled in Table 1. ^{1}H-NMR spectra of molecules **1**, **2**, **3**, **5** and **6** in DMSO solvent are reported in the ESI† (Fig. S12–S16).

From the ^{1}H-NMR chemical shift data reported in Table 1, the role of the intramolecular HB in controlling the conformational populations is apparent. As soon as the intramolecular HB breaks in the high polar DMSO solvent, the population of conformer **II** increases for molecule **2**, whereas molecule **5**, which existed as a single conformer **I** in $CDCl_3$ solvent (because of the strong intramolecular HB), reveals both conformers **I** and **II** upon rupture of the intramolecular HB in DMSO solvent (Table 1).

Temperature perturbation study

The strengths of most of the non-covalent interactions like HB increases on decreasing the temperature. Consequently, the shift of the proton resonance frequency towards the low field indicates the presence of HB.[42,45] The temperature dependent changes in the chemical shifts for compounds **1–6** are compiled in Fig. 8. For molecule **1** and the conformer **II** of molecules **3** and **6**, larger deshielding is observed, indicating the substantial strengthening of the HB, which is possible only when the NH proton is involved in the intermolecular HB as there is no structural barrier for the molecules to come closer upon strengthening of the HB. Another interesting observation on lowering the temperature is the increase in the intensity of one of the two NH proton peaks at the expense of the intensity of the other NH proton peak of molecule **3** (Fig. S17, ESI†) due to the strengthening of the intramolecular HB, which also unequivocally establishes that the strength of the HB controls the conformational populations in these molecules.

The changes in the NH proton chemical shifts observed from the titration studies are summarised in Table 2.

Energy of intramolecular HBs (X···H–N)

For all the investigated compounds, the energies of the HB (E_{HB}) were calculated using an empirical relation $E_{HB} = \Delta\delta + (0.4 \pm 0.2)$ (kcal mol^{-1}),[46–48] where $\Delta\delta$ represents the chemical shift difference between the hydrogen bonded proton and the free proton. In the present work, the $\Delta\delta$ values are calculated by subtracting δ_{NH} of molecule **1** from δ_{NH} of molecules **2**, **3**, **5** and **6**. Since there is no intramolecular HB in conformer **II**, the E_{HB} values are calculated for conformer **I** and are compiled in Table 3. For conformer **I**, these values vary from 0 to 1.6 kcal mol^{-1}, showing

Table 1 ^{1}H-NMR chemical shifts of the NH imide and CH vinyl protons for the *trans*, E_{C-N} (**I**)/*cis*, E_{C-N} (**II**) conformers of molecules **1**, **2**, **3**, **5** and **6** in $CDCl_3$ and DMSO solvents

		NH (δ in ppm)		CH (δ in ppm)			Conformer % in	
Molecule	X	$CDCl_3$	DMSO	$CDCl_3$	DMSO	Conformer	$CDCl_3$	DMSO
1	H	9.22	11.84	8.35	8.47	**I**	100	100
		—	—	—	—	**II**	—	—
2	F	9.67	11.83	8.26	8.33	**I**	90	71
		9.16	11.95	—	8.07	**II**	10	29
3	Cl	9.25	11.90	8.30	8.28	**I**	48	64
		10.07	11.96	7.95	8.06	**II**	52	36
5	OMe	10.83	11.46	8.28	8.35	**I**	100	84
		—	11.63	—	8.00	**II**	—	16
6	CF_3	8.83	11.96	8.23	8.28	**I**	33	58
		9.84	12.01	7.82	8.04	**II**	67	42

Table 2 The temperature and solvent dependent NH proton chemical shift variations for compounds **1**, **2**, **3**, **5** and **6**

		Change in chemical shift (ppm)					
		On adding 600 μl $CDCl_3$		On adding 250 μl DMSO		Temperature varied from 298 to 220 K	
Molecule	Substituent X	I	II	I	II	I	II
1	H	−0.0794	—	4.6317	—	1.4332	—
2	F	−0.0095	—	2.0705	—	0.2398	—
3	Cl	−0.0293	−0.2974	2.7381	2.3568	0.5096	2.3659
5	OMe	0.0214	—	0.5525	—	0.3100	—
6	CF_3	−0.0324	−0.3206	3.1429	2.4299	0.7556	2.4245

Table 3 Δ_{NH} and E_{HB} values for conformer **I** of compounds **2**, **3**, **5** and **6**

		δ_{NH} in the solvent $CDCl_3$ (ppm)	Difference in δ_{NH} with respect to molecule **1**	Energy of HB (E_{HB}) (kcal mol^{-1})
Molecule	Substituent X	I	I	I
1	H	9.22	—	—
2	F	9.67	0.45	0.8
3	Cl	9.25	0.03	0.4
5	OMe	10.83	1.16	1.6
6	CF_3	8.83	−0.39	0.0

the presence of weak C–X···H–N type HB interactions in molecules **2**, **3**, **5** and no C–X···H–N type HB interaction for molecule **6**.

Detection of HB mediated coupling

The symbolic representation of the hydrogen bond mediated coupling is $^{nh}J_{XY}$, where X and Y are coupled nuclei and the superscript nh represents the number of bonds separating the interacting nuclei through hydrogen bonds and covalent bonds. The NH proton of molecule **2** showed a doublet due to its coupling with the fluorine atom (Fig. 9a). The interaction between these two atoms is confirmed by $^1H\{^{19}F\}$ (fluorine decoupled) spectra in the $CDCl_3$ solvent,[44] and the corresponding spectrum is reported in Fig. 9b. The coupling of nearly 14 Hz between ^1H and ^{19}F was detected, which are separated by several (5) bonds. Such a large value is unexpected for $^5J_{FH}$ and can be attributed to the direct interaction between ^{19}F and ^1H ($^{1h}J_{FH}$), where the transfer of spin polarization between them is mediated through HB, giving an explicit evidence for the presence of HB between them.[49–51] This is also confirmed by the collapse of the doublet into a singlet in DMSO-d_6 solvent, where the HB is broken. The corresponding spectrum is shown in Fig. 9c. Another interesting observation from the ^1H NMR spectrum of molecule **2** is that the ratio of the two conformation

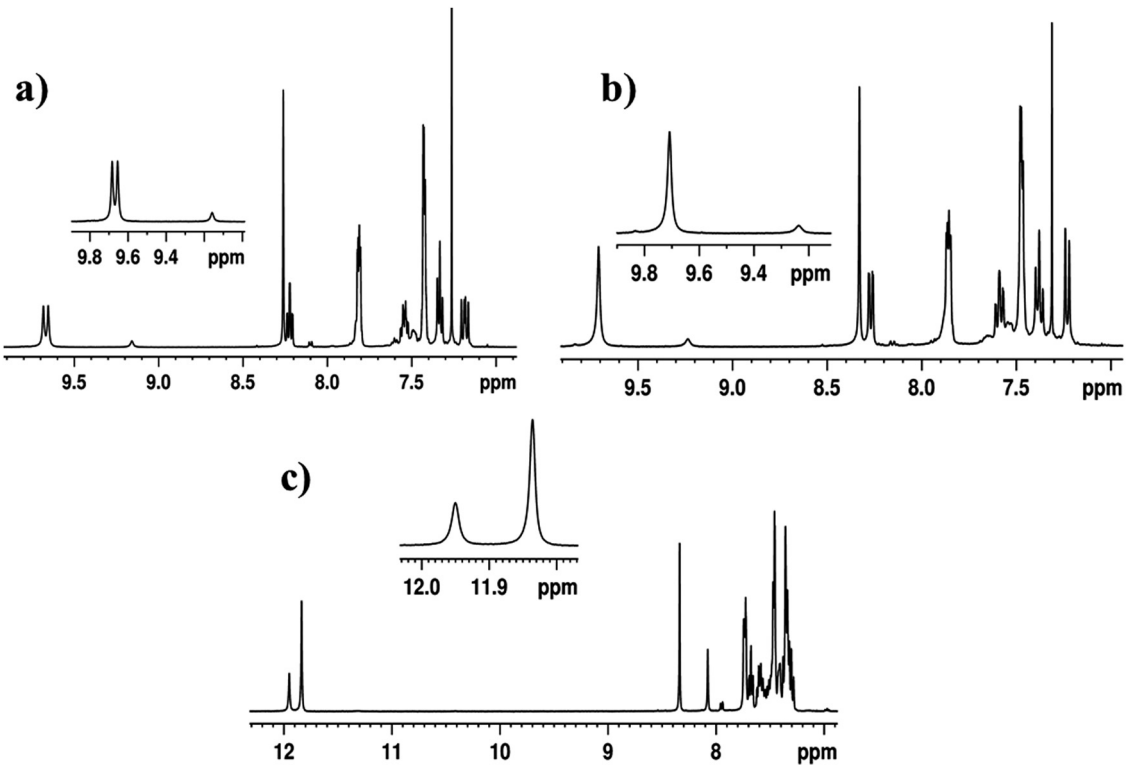

Fig. 9 400 MHz (a) ^1H spectrum of compound **2** in $CDCl_3$ solvent, (b) $^1H\{^{19}F\}$ spectrum in $CDCl_3$ solvent (c) ^1H spectrum of compound **2** in DMSO-d_6 solvent. Two peaks pertaining to NH are expanded in the inset given.

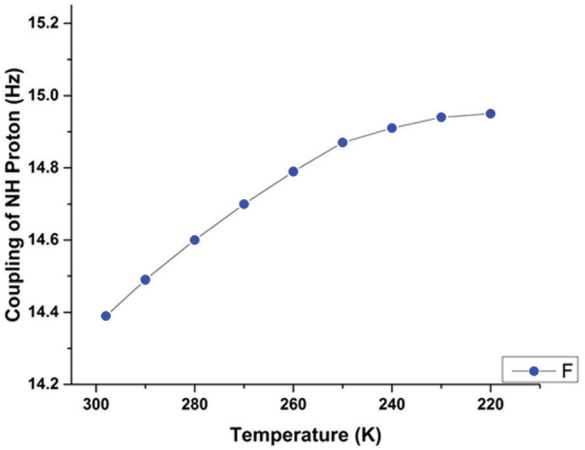

Fig. 10 Temperature dependent changes in the $^{1h}J_{NH}$ for molecule **2**. The experiment was performed using $CDCl_3$ solvent at 10 mM concentration and the temperature was varied from 300 K to 220 K.

populations is nearly 90 : 10 in the solvent $CDCl_3$, which drastically decreases to 79 : 21 (Table 1) in the solvent DMSO-d_6 as the intramolecular HB ruptures. This unequivocally establishes that the organic fluorine mediated intramolecular HB is controlling the 90% of the population for conformer **I** in the solvent $CDCl_3$ (Fig. 9a).

Variation of $^{1h}J_{FH}$ with temperature

The covalent bond mediated couplings are invariant for a particular conformation, and if the conformation is flexible, one would get the average value of the coupling constant pertaining to the possible geometries. Fig. 10 shows the change in $^{1h}J_{FH}$ as a function of temperature for compound **2**. The steady increase in the coupling constant from 14.4 Hz to 15 Hz on lowering the temperature from 298 K to 220 K supports the presence of HB mediated coupling. This is attributed to the decrease in the distance between the NH proton and the F atom upon strengthening of the HB.

Computational details

The weak molecular interactions in the investigated molecules established by NMR experiments were further ascertained by Density Functional Theory (DFT)[52,53] based Non-Covalent Interaction (NCI)[54] and Quantum Theory of Atoms in Molecules (QTAIM)[55] studies. All the computational modelling were performed using Gaussian09 program,[56] choosing a DFT method at the B3LYP/6-311g(d,p) level of theory and chloroform as a default solvent. The optimized minimum energy structures were confirmed by harmonic vibrational frequency values. With the help of the optimized structure coordinates, the wave function files for the QTAIM and NCI studies were

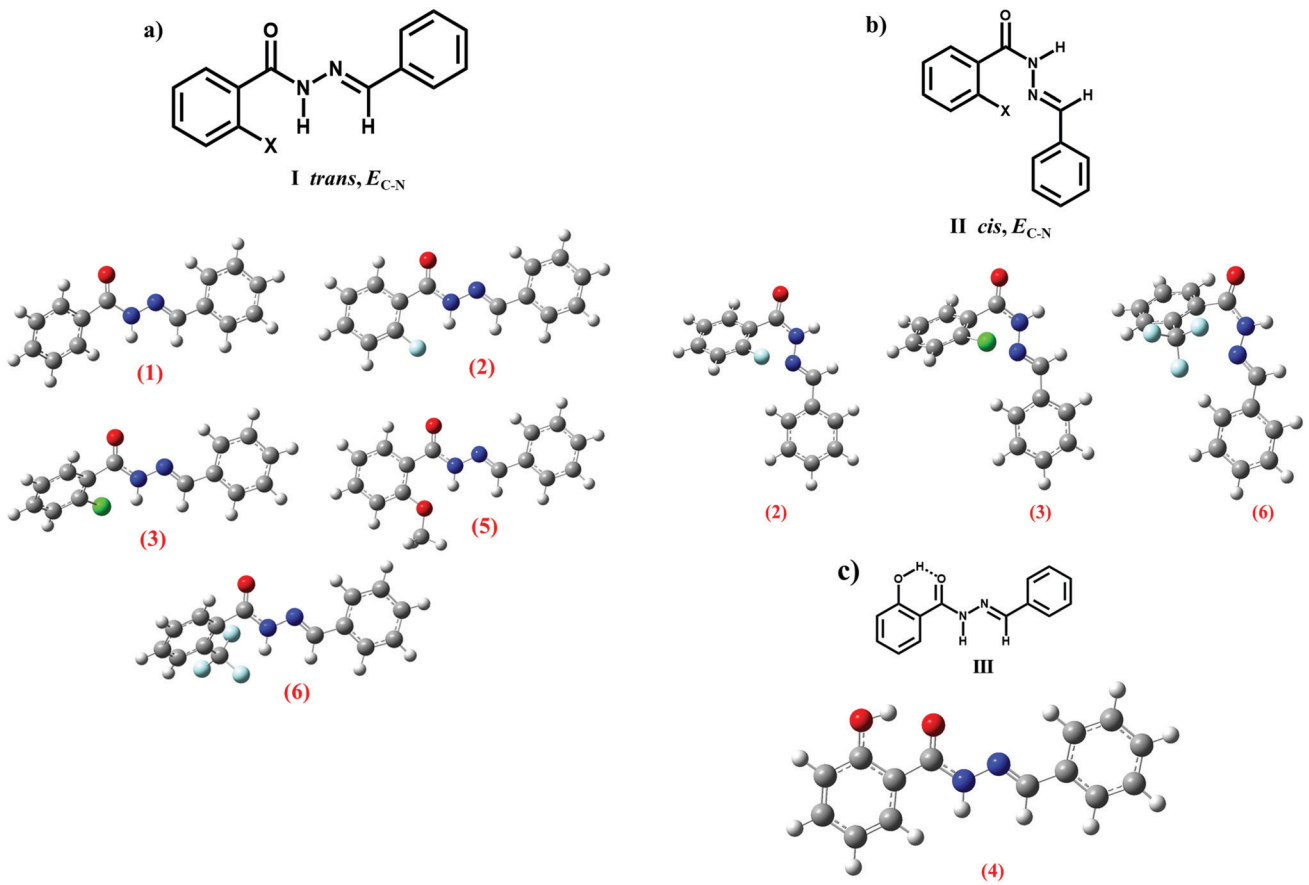

Fig. 11 The DFT optimized spatial structure; (a) for conformer **I** (*trans*, E_{C-N}) of molecules **1**, **2**, **3**, **5** and **6**; (b) for conformer **II** (*cis*, E_{C-N}) of molecules **2**, **3** and **6**; (c) for conformer **III** of molecule **4**.

Table 4 Gibbs free energy for conformers **I** and **II** and calculated bond geometries for conformer **I** of molecules **2**, **3**, **5** and **6**

		Gibbs free energy of molecules in conformers (kJ mol^{-1})		Distance $d_{X\cdots HN}$ (Å)	Angle XHN (°)
Molecule	HB type (X···HN)	**I**	**II**	**I**	**I**
1	(H···HN)	−1905104.9415973	—	—	—
2	(F···HN)	−2165724.3073241	−2165716.7224903	1.925	132.6
3	(Cl···HN)	−3111825.21609953	−3111826.69948089	2.693	107.2
5	(MeO···HN)	−2205874.4711383	—	1.863	134.1
6	(CF_3···HN)	−2790244.90184566	−2790244.5760736	2.218	126.8

generated. Detailed discussion on the theoretical computations is provided in the ESI.† The optimized spatial structures considering the possible electron resonance of all the conformers of molecules **1–6** are reported in Fig. 11. The extracted Gibbs free energies of both the optimised conformations of the studied molecules along with the bond geometries, specifically the distances and angles for conformer **I** (no intramolecular HB in conformer **II**) of molecules **2**, **3**, **5** and **6** are compiled in Table 4.

Conclusions

The NMR investigations on the series of synthesized molecules containing the azomethine group (–N=C<) with different substitutions on the benzoyl ring of *N*′-benzylidenebenzohydrazide revealed several interesting results; (a) the correlated cross peaks in the 2D NOESY spectrum confirm that the molecules exist as only *E* isomers with respect to the C=N bond, (b) most of them exist in *trans*/*cis* conformations around the N–C(O) bond; (c) single intramolecular HB between different substituents on the benzoyl ring including organic fluorine, and the proton of the amide group (C–X···H–N) is controlling the conformational rigidity by establishing the intramolecular HB; and (d) the conformer populations are strongly dependent on the strength of the HB. We envisage that the strength of the intramolecular HB can be manipulated for the architectural design of the molecule to a single conformation instead of possible multiple conformations or conformers of the desired ratio. The participation of organic fluorine in the HB has been demonstrated by detection of $^{1h}J_{HF}$ and its disappearance upon decoupling with ^{19}F and also in a high polarity solvent.

Conflicts of interest

There are no conflicts to declare.

Acknowledgements

NA is grateful to the Indian Institute of Science for the SRF. SKM thank the Indian Institute of Science for the RA position. NS gratefully acknowledges the generous financial support by the Science and Engineering Research Board (SERB), New Delhi (Grant Number: CRG/2018/002006).

References

1 W.-H. Hu, K. W. Huang, C.-W. Chiou and S.-W. Kuo, *Macromolecules*, 2012, **45**, 9020.
2 M. Saccone, V. Dichiarante, A. Forni, A. Goulet-Hanssens, G. Cavallo, J. Vapaavuori, G. Terraneo, C. J. Barrett, G. Resnati, P. Metrangolo and A. Priimagi, *J. Mater. Chem. C*, 2015, **3**, 759.
3 L. Brunsveld, B. J. B. Folmer, E. W. Meijer and R. P. Sijbesma, *Chem. Rev.*, 2001, **101**, 4071.
4 F. Huang and H. W. Gibson, *Prog. Polym. Sci.*, 2005, **30**, 982; O. Lukin and F. Vögtle, *Angew. Chem., Int. Ed.*, 2005, **44**, 1456.
5 O. Lukin and F. Vögtle, *Angew. Chem., Int. Ed.*, 2005, **44**, 1456.
6 R. Shenhar and V. M. Rotello, *Acc. Chem. Res.*, 2003, **36**, 549.
7 R. P. Sijbesma and E. W. Meijer, *Chem. Commun.*, 2003, 5.
8 B. Gong, *Chem. – Eur. J.*, 2001, **7**, 4336.
9 J. W. Lockman, N. M. Paul and J. R. Parquette, *Prog. Polym. Sci.*, 2005, **30**, 423.
10 I. Muegge, S. L. Heald and D. Brittelli, *J. Med. Chem.*, 2001, **44**, 1841.
11 B. E. Smart, *J. Fluorine Chem.*, 2001, **109**, 3.
12 G. R. Desiraju, *J. Am. Chem. Soc.*, 2013, **135**, 9952.
13 R. Berger, G. Resnati, P. Metrangolo, E. Weber and J. Hulliger, *Chem. Soc. Rev.*, 2011, **40**, 3496.
14 R. Banerjee, G. R. Desiraju, R. Mondal and J. A. K. Howard, *Chem. – Eur. J.*, 2004, **10**, 3373.
15 C. Li, S.-F. Ren, J.-L. Hou, H.-P. Yi, S.-Z. Zhu, X.-K. Jiang and Z.-T. Li, *Angew. Chem., Int. Ed.*, 2005, **44**, 5725.
16 X. Zhao, X.-Z. Wang, X.-K. Jiang, Y.-Q. Chen, Z.-T. Li and G.-J. Chen, *J. Am. Chem. Soc.*, 2003, **125**, 15128.
17 M. D. Struble, C. Kelly, M. A. Siegler and T. Lectka, *Angew. Chem., Int. Ed.*, 2014, **126**, 9070.
18 C. Dalvita and A. Vulpetti, *Chem. – Eur. J.*, 2016, **22**, 7592.
19 G. T. Giuffredi, V. Gouverneur and B. Bernet, *Angew. Chem., Int. Ed.*, 2013, **125**, 10718.
20 S. K. Mishra and N. Suryaprakash, *Molecules*, 2017, **22**, 423.
21 D. O'Hagan and H. S. Rzepa, *Chem. Commun.*, 1997, 645.
22 L. H. Takahashi, R. Radhakrishnan, R. E. Rosenfield, E. F. Meyer and D. A. Trainor, *J. Am. Chem. Soc.*, 1989, **111**, 3368.
23 L. Hunter, *Beilstein J. Org. Chem.*, 2010, **6**, 38.
24 A. Walcourt, M. Loyevsky, D. B. Lovejoy, V. R. Gordeuk and D. R. Richardson, *Int. J. Biochem. Cell Biol.*, 2004, **36**, 401.
25 K. L. Vine, J. M. Locke, M. Ranson, S. G. Pyne and J. B. Bremner, *J. Med. Chem.*, 2007, **50**, 5109.
26 A. M. Asiri and S. A. Khan, *Molecules*, 2010, **15**, 6850.
27 C. Amutha, S. Sarvanan and S. Muthusubhramanian, *Indian J. Chem.*, 2014, **53B**, 337.
28 P. Panneerselvam, R. R. Nair, G. Vijayalakshmi, E. H. Subramanian and S. K. Sridhar, *Eur. J. Med. Chem.*, 2005, **40**, 225.

29 A. Jarrahpour, D. Khalili, E. D. Clercq, C. Salmi and J. M. Brunel, *Molecules*, 2007, **12**, 1720.
30 T. Ren, J. Wang, G. Li and Y. Li, *Asian J. Chem.*, 2014, **26**, 8309.
31 K. F. Morris and C. S. Johnson, *J. Am. Chem. Soc.*, 1992, **114**, 3139.
32 H. Schiff, *Justus Liebigs Ann. Chem.*, 1864, **131**, 118.
33 K. F. Morris and C. S. Johnson, *J. Am. Chem. Soc.*, 1993, **115**, 4291.
34 C. Yu and G. C. Levy, *J. Am. Chem. Soc.*, 1984, **106**, 6533.
35 G. Palla, G. Predieri, P. Domiano, C. Vignali and W. Turner, *Tetrahedron*, 1986, **42**, 3649.
36 G. Palla, C. Pelizzi, G. Predieri and C. Vignali, *Gazz. Chim. Ital.*, 1982, **112**, 339.
37 L. E. Zimmer, C. Sparr and R. Gilmour, *Angew. Chem., Int. Ed.*, 2011, **50**, 11860.
38 A. K. Jissy and A. Datta, *J. Phys. Chem. B*, 2010, **114**, 15311.
39 C. Bartolomé, P. Espinet and J. M. Martín-Alvarez, *Chem. Commun.*, 2007, 4384.
40 S. K. Mishra and N. Suryaprakash, *Phys. Chem. Chem. Phys.*, 2015, **17**, 15226.
41 S. H. Gellman, B. R. Adams and G. P. Dado, *J. Am. Chem. Soc.*, 1990, **112**, 460.
42 S. K. Mishra and N. Suryaprakash, *RSC Adv.*, 2015, **5**, 86013.
43 P. Dhanishta, S. K. Mishra and N. Suryaprakash, *J. Phys. Chem. A*, 2018, **122**, 199.
44 F. J. Martinez-Martinez, A. Ariza-Castolo, H. Tlahuext, M. Tlahuextl and R. Contreras, *J. Chem. Soc., Perkin Trans. 2*, 1993, 1481.
45 W. Kohn and L. J. Sham, *Phys. Rev.*, 1965, **140**, A1133.
46 D. Rusinska-Roszak, *J. Phys. Chem. A*, 2015, **119**, 3674.
47 A. V. Afonin, A. V. Vashchenko and M. V. Sigalov, *Org. Biomol. Chem.*, 2016, **14**, 11199.
48 A. J. Dingley, J. E. Masse, R. D. Peterson, M. Barfield, J. Feigon and S. Grzesiek, *J. Am. Chem. Soc.*, 1999, **121**, 6019.
49 A. Dunger, H.-H. Limbach and K. Weisz, *J. Am. Chem. Soc.*, 2000, **122**, 10109.
50 S. Grzesiek, F. Cordier, V. Jaravine and M. Barfield, *Prog. Nucl. Magn. Reson. Spectrosc.*, 2004, **45**, 275.
51 J. Contreras-García, W. Yang and E. R. Johnson, *J. Phys. Chem. A*, 2011, **115**, 12983.
52 R. G. Parr and W. Yang, *Density-Functional Theory of Atoms and Molecules*, Oxford University Press, New York, 1989.
53 J. R. Cheeseman, G. W. Trucks, T. A. Keith and M. J. Frisch, *J. Chem. Phys.*, 1996, **104**, 5497.
54 R. F. W. Bader, S. G. Anderson and A. J. Duke, *J. Am. Chem. Soc.*, 1979, **101**, 1389–1395.
55 R. F. W. Bader, *Atoms in Molecules: A Quantum Theory*, Oxford University Press, Oxford, 1990.
56 M. J. Frisch, G. W. Trucks, H. B. Schlegel, G. E. Scuseria, M. A. Robb, J. R. Cheeseman, G. Scalmani, V. Barone, B. Mennucci, G. A. Petersson, H. Nakatsuji, M. Caricato, X. Li, H. P. Hratchian, A. F. Izmaylov, J. Bloino, G. Zheng, J. L. Sonnenberg, M. Hada, M. Ehara, K. Toyota, R. Fukuda, J. Hasegawa, M. Ishida, T. Nakajima, Y. Honda, O. Kitao, H. Nakai, T. Vreven, J. A. Montgomery Jr, J. E. Peralta, F. Ogliaro, M. J. Bearpark, J. Heyd, E. N. Brothers, K. N. Kudin, V. N. Staroverov, R. Kobayashi, J. Normand, K. Raghavachari, A. P. Rendell, J. C. Burant, S. S. Iyengar, J. Tomasi, M. Cossi, N. Rega, N. J. Millam, M. Klene, J. E. Knox, J. B. Cross, V. Bakken, C. Adamo, J. Jaramillo, R. Gomperts, R. E. Stratmann, O. Yazyev, A. J. Austin, R. Cammi, C. Pomelli, J. W. Ochterski, R. L. Martin, K. Morokuma, V. G. Zakrzewski, G. A. Voth, P. Salvador, J. J. Dannenberg, S. Dapprich, A. D. Daniels, Ö. Farkas, J. B. Foresman, J. V. Ortiz, J. Cioslowski and D. J. Fox, *Gaussian09*, Gaussian, Inc., Wallingford, CT, USA, 2009.